Article:

Trodden, P., Bukhsh, W., Grothey, A. et al. (1 more author) (2013) MILP formulation for controlled islanding of power networks. International Journal of Electrical Power and Energy Systems, 45 (1). 501 - 508. ISSN 0142-0615

https://doi.org/10.1016/j.ijepes.2012.09.018

MILP formulation for controlled islanding of power networks☆

P. A. Trodden[a,*], W. A. Bukhsh[a], A. Grothey[a], K. I. M. McKinnon[a]

[a]*School of Mathematics, University of Edinburgh, James Clerk Maxwell Building, King's Buildings, Mayfield Road, Edinburgh EH9 3JZ, United Kingdom*

Abstract

This paper presents a flexible optimization approach to the problem of intentionally forming islands in a power network. A mixed integer linear programming (MILP) formulation is given for the problem of deciding simultaneously on the boundaries of the islands and adjustments to generators, so as to minimize the expected load shed while ensuring no system constraints are violated. The solution of this problem is, within each island, balanced in load and generation and satisfies steady-state DC power flow equations and operating limits. Numerical tests on test networks up to 300 buses show the method is computationally efficient. A subsequent AC optimal load shedding optimization on the islanded network model provides a solution that satisfies AC power flow. Time-domain simulations using second-order models of system dynamics show that if penalties were included in the MILP to discourage disconnecting lines and generators with large flows or outputs, the actions of network splitting and load shedding did not lead to a loss of stability.

Keywords: optimization, integer programming, controlled islanding, blackouts

1. Introduction

In recent years, there has been an increase in the occurrence of wide-area blackouts of power networks. In 2003, separate blackouts in Italy [1], Sweden/Denmark [2] and USA/Canada [3] affected millions of customers. The wide-area disturbance in 2006 to the European system caused

☆This work is supported by the UK Engineering and Physical Sciences Research Council (EPSRC) under grant EP/G060169/1.

*Corresponding author. Tel. +44-131-650-5055. Fax +44-131-650-6553.

Email addresses: paul.trodden@ed.ac.uk (P. A. Trodden), w.a.bukhsh@sms.ed.ac.uk (W. A. Bukhsh), a.grothey@ed.ac.uk (A. Grothey), k.mckinnon@ed.ac.uk (K. I. M. McKinnon)

the system to split in an uncontrollable way [4], forming three islands. More recently, the UK network experienced a system-wide disturbance caused by an unexpected loss of generation; blackout was avoided by local load shedding [5].

While the exact causes of wide-area blackouts differ from case to case, some common driving factors emerge. Modern power systems are being operated closer to limits: liberalization of the markets, and the subsequent increased commercial pressures and change in expenditure priorities, has led to a reduction in security margins [6, 7, 8]. A more recently occurring factor is increased penetration of variable distributed generation, notably from wind power, which brings significant challenges to secure system operation [9].

For several large disturbance events, *e.g.*, [3], studies have shown that a wide-area blackout could have been prevented by intentionally splitting the system into islands [10]. By isolating the faulty part of the network, the total load disconnected in the event of a cascading failure is reduced. *Controlled islanding* or *system splitting* is therefore attracting an increasing amount of attention. The problem is how to split the network into islands that are as closely balanced as possible in load and generation, have stable steady-state operating points within voltage and line limits, and so that the action of splitting does not cause dynamic instability. This is a considerable challenge, since the search space of line cutsets grows exponentially with network size, and is exacerbated by the requirement for strategies that obey non-linear power flow equations and satisfy operating constraints.

It is not computationally practical to tackle all these aspects of the problem simultaneously within a single optimization, and approaches in the literature differ according to which aspect is treated as the primary objective. Additionally different search methods have been proposed for defining the island boundaries. An example where the primary objective is to produce load balanced islands is [11]. This proposes a three-phase ordered binary decision diagram (OBDD) to generate a set of islanding strategies. The approach uses a reduced graph-theoretical model of the network to minimize the search space for islanding; power flow analyses are subsequently executed on islands to exclude strategies that violate operating constraints, *e.g.*, line limits.

In other approaches the primary objective is to split the network into electromechanically stable islands, commonly by splitting so that generators with coherent oscillatory modes are grouped.

If the system can be split along boundaries of coherent generator groups while not causing excessive imbalance between load and generation, then the system is less likely to lose stability. Determining the required cutset of lines involves, as a secondary objective, considerations of load-generation balance and other constraints; algorithms include exhaustive search [12], minimal-flow minimal-cutset determination using breadth-/depth-first search [13], graph simplification and partitioning [14], and metaheuristics [15, 16]. The authors of [17] propose a framework that, iteratively, identifies the controlling group of machines and the contingencies that most severely impact system stability, and uses a heuristic method to search for a splitting strategy that maintains a desired stability margin. Wang et al. [18] employed a power flow tracing algorithm to first determine the domain of each generator, *i.e.*, the set of load buses that 'belong' to each generator. Subsequently, the network is coarsely split along domain intersections before refinement of boundaries to minimize imbalances.

The current paper presents an optimization framework for controlled islanding. The method's primary objective is to minimize the expected amount of load that has to be disconnected while leaving the islanded network in a balanced steady state. The post-islanding dynamics are not modelled explicitly in the optimization, as this greatly increases the computational difficulty of the problem. Instead penalties are used to discourage large changes to power flows, and it is shown by simulation that this results in the islanding solutions being dynamically stable.

The proposed approach has two stages: first, a mixed-integer linear programming (MILP) islanding problem, which includes the linear DC flow equations and flow limits, is solved to determine a DC-feasible solution; secondly, an AC optimal load shedding optimization is solved to provide an AC-feasible steady-state post-islanding operating point. Integer programming has many applications in power systems, but its use in network splitting and blackout prevention is limited. Bienstock and Mattia [19] proposed an IP-based approach to the problem of designing networks that are robust to sets of cascading failures and thus avoid blackouts; whether to upgrade a line's capacity is a binary decision. Fisher et al. [20], Khodaei and Shahidehpour [21] propose methods for optimal transmission switching for the problem of minimizing the cost of generation dispatch by selecting a network topology to suit a particular load. In common with the formulation presented here, binary variables represent switches that open or close each line and the DC power flow model is used, resulting in a MILP problem. However, in the current paper sectioning constraints are present, and the problem is to design balanced islands while minimizing load shed.

The organization of the paper is as follows. The next section outlines the motivation and assumptions that underpin the approach. The DC MILP islanding formulation is developed in Section 3. The AC optimal load shedding problem is described in Section 4. In Section 5 computational results are presented. In Section 6, the dynamic stability of the networks in response to islanding is investigated. Finally, conclusions are drawn in Section 7.

2. Motivation

An application of islanding which has received little attention is islanding in response to particular contingencies so as to isolate vulnerable parts of the network. For example after some failure, part of the network may be vulnerable to further failure, or a suspected failure of monitoring equipment may have resulted in the exact state of part of the network being uncertain. In such a case an action that would prevent cascading failures throughout the network is to form an island surrounding the uncertain part of the network so isolating it from the rest. A method that does not take into account the location of the trouble when designing islands may leave the uncertain equipment within a large section of the network, all of which may become insecure as a result. Figure 1(a) illustrates the situation: uncertain lines and buses are indicated by a "?". Figure 1(b) shows a possible islanding solution for this network: all uncertain buses have been placed in Section 0 and all uncertain lines with at least one end in Section 1 are disconnected. The following distinction is made between *sections* and *islands*. The split network consists of two sections, an "unhealthy" Section 0 and a "healthy" Section 1 with no lines connecting the two sections, and all uncertain equipment in Section 0. However, neither section is required to be connected so may contain more than one island: in Figure 1(b), Section 1 comprises islands 1, 3 and 4, and Section 0 is a single island. The optimization will determine the boundaries of the sections, the number and boundaries of the islands, the generator adjustments, and the amount of each load that is planned to be shed.

A balance has to be found between the load that is planned to be shed and the residual load that is left in Section 0, which may be lost because that section is vulnerable. This can be achieved by taking as objective the sum of the value of the loads remaining in both sections after the planned

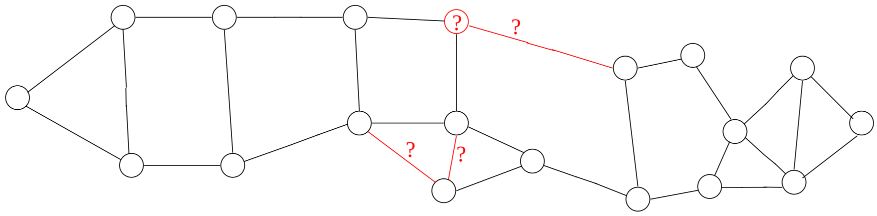

(a) Network prior to islanding

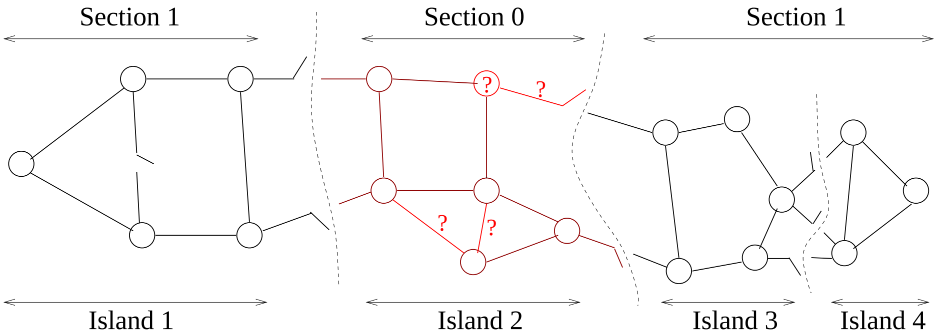

(b) Network post islanding

Figure 1: (a) Illustration of a network with uncertain buses and lines, and (b) the islanding of that network by disconnecting lines.

load shedding minus a proportion of the the value of the load remaining in Section 0 after the planned load is shed.

3. MILP islanding formulation

This section presents a MILP formulation for the problem of finding a steady state islanded solution in a stressed network, while minimizing the expected load lost.

Consider a network that comprises a set of buses $\mathcal{B} = \{1, 2, \ldots, n^{\mathrm{B}}\}$ and a set of lines $\mathcal{L}$. The two vectors F and T describe the connection topology of the network: a line $l \in \mathcal{L}$ connects bus F_l to bus T_l. There exists a set of generators $\mathcal{G}$ and a set of loads $\mathcal{D}$. A subset $\mathcal{G}_b$ of generators is attached to bus $b \in \mathcal{B}$; similarly, $\mathcal{D}_b$ contains the subset of loads present at bus $b \in \mathcal{B}$.

3.1. Sectioning constraints

Motivated by the previous section, the intention is to partition the buses and lines between Sections 0 and 1. It is suspected that some subset $\mathcal{B}^0 \subseteq \mathcal{B}$ of buses and some subset $\mathcal{L}^0 \subseteq \mathcal{L}$ of lines are faulty or at risk. No uncertain components are allow in Section 1.

A binary variable γ_b is defined for each bus $b \in \mathcal{B}$; γ_b is set equal to 0 if b is placed in section 0 and $\gamma_b = 1$ otherwise. A binary variable ρ_l is defined for each $l \in \mathcal{L}$; $\rho_l = 0$ if line l is disconnected and $\rho_l = 1$ otherwise.

Constraints (1a) and (1b) apply to lines in $\mathcal{L} \setminus \mathcal{L}^0$. A line is cut if its two end buses are in different sections (*i.e.* $\gamma_{F_l} = 0$ and $\gamma_{T_l} = 1$, or $\gamma_{F_l} = 1$ and $\gamma_{T_l} = 0$). Otherwise, if the two end buses are in the same section then $\rho_l \leq 1$, and the line may or may not be disconnected. Thus, these constraints enforce the requirement that any certain line between sections 0 and 1 shall be disconnected.

$$\rho_l \leq 1 + \gamma_{F_l} - \gamma_{T_l}, \forall l \in \mathcal{L} \setminus \mathcal{L}^0, \tag{1a}$$

$$\rho_l \leq 1 - \gamma_{F_l} + \gamma_{T_l}, \forall l \in \mathcal{L} \setminus \mathcal{L}^0. \tag{1b}$$

Constraints (1c) and (1d) apply to lines assigned to $\mathcal{L}^0$. A line $l \in \mathcal{L}^0$ is disconnected if at least one of the ends is in Section 1. Thus, an uncertain line either (i) shall be disconnected if entirely in Section 1, (ii) shall be disconnected if between sections 0 and 1, or (iii) may remain connected if entirely in Section 0.

$$\rho_l \leq 1 - \gamma_{F_l}, \forall l \in \mathcal{L}^0, \tag{1c}$$

$$\rho_l \leq 1 - \gamma_{T_l}, \forall l \in \mathcal{L}^0, \tag{1d}$$

Constraints (1e) and (1f) set the value of γ_b for a bus b depending on what section that bus was assigned to. $\mathcal{B}^1$ is defined as the set of buses that are required to remain in Section 1. It may be desirable to exclude buses from the “unhealthy” section, and such an assignment will usually reduce computation time.

$$\gamma_b = 0, \forall b \in \mathcal{B}^0, \tag{1e}$$

$$\gamma_b = 1, \forall b \in \mathcal{B}^1. \tag{1f}$$

Given some assignments to $\mathcal{B}^0, \mathcal{B}^1$ and $\mathcal{L}^0$, the optimization will disconnect lines and place buses in Sections 0 or 1, hence partitioning the network into Sections 0 and 1. What else is placed in Section 0, what other lines are cut, and which loads and generators are adjusted, are degrees of freedom for the optimization, and will depend on the objective function.

3.2. *DC power flow model with line losses*

The power flow model employed is a variant of the "DC" model. As in the standard DC model it assumes unit voltage at each bus and uses a linearization of Kirchhoff's voltage law (KVL), but unlike the standard DC model the variant also accounts for line losses. Kirchhoff's current law is applied at each bus $b \in \mathcal{B}$:

$$\sum_{g \in \mathcal{G}_b} p_g^{\mathrm{G}} = \sum_{d \in \mathcal{D}_b} p_d^{\mathrm{D}} + \sum_{l \in \mathcal{L}: F_l = b} p_l^{\mathrm{L}} - \sum_{l \in \mathcal{L}: T_l = b} (p_l^{\mathrm{L}} - \overline{h}_l^{\mathrm{L}}), \tag{2}$$

where p_g^{G} is the real power output of generator $g \in \mathcal{G}_b$ at bus b, p_d^{D} is the real power demand from load $d \in \mathcal{D}_b$. The variable p_l^{L} is the real power flow from bus F_l into the first end of line l, and $p_l^{\mathrm{L}} - \overline{h}_l^{\mathrm{L}}$ is the flow out of the second end of line l into bus T_l, the difference in the flows being the loss $\overline{h}_l^{\mathrm{L}}$.

The standard DC model has no line loss, *i.e.*, $\overline{h}_l^{\mathrm{L}} = 0$, but this model results in the load loss being underestimated. Actual line losses are non-linear functions of voltages and phase angle differences, and these can be approximated in the DC model by a piecewise linear function. However investigations have shown that this offers little or no improvement in the objective over a simple constant-loss approximation, but adversely affects computation [22]. In this paper, therefore, a constant loss model is employed. The loss for line l is given by

$$\overline{h}_l^{\mathrm{L}} = \rho_l h_l^{\mathrm{L0}}, \tag{3}$$

where h_l^{L0} is the loss immediately before islanding. The inclusion of ρ_l drives the loss to zero if the islanding optimization cuts the line.

The linearized version of Kirchhoff's voltage law (KVL) has the form

$$\hat{p}_l^{\mathrm{L}} = -B_l^{\mathrm{L}}(\delta_{F_l} - \delta_{T_l}), \tag{4}$$

where B_l^{L} is the susceptance of line l and $\hat{p}_l^{\mathrm{L}}$ an auxiliary variable for the real power flow. When the line l is connected then it is required that $p_l^{\mathrm{L}} = \hat{p}_l^{\mathrm{L}}$, but when it is disconnected then $p_l^{\mathrm{L}} = 0$ and $\hat{p}_l^{\mathrm{L}}$ is free. This is modelled as follows.

$$-\rho_l P_l^{\mathrm{Lmax}} \leq p_l^{\mathrm{L}} \leq P_l^{\mathrm{Lmax}} \rho_l, \tag{5a}$$

$$-(1 - \rho_l)\hat{P}_l^{\mathrm{Lmax}} \leq \hat{p}_l^{\mathrm{L}} - p_l^{\mathrm{L}} \leq \hat{P}_l^{\mathrm{Lmax}}(1 - \rho_l), \tag{5b}$$

where P_l^{Lmax} is the maximum possible magnitude of real power flow through a line l, and $\hat{P}_l^{\text{Lmax}}$ should be large enough to allow two buses across a disconnected line to maintain sufficiently different phase angles. (Note that at the very minimum $\hat{P}_l^{\text{Lmax}} \geq P_l^{\text{Lmax}}$.) If $\rho_l = 0$, then $p_l^{\text{L}} = 0$ but $\hat{p}_l^{\text{L}}$ may take whatever value is necessary to satisfy the KVL constraint (4), while if $\rho_l = 1$ then $p_l^{\text{L}} = \hat{p}_l^{\text{L}}$.

Line limits P_l^{Lmax} may be expressed either directly as MW ratings on real power for each line, or as a limit on the phase angle difference across a line. Since in the model the real power through a line is just a simple scaling of the phase difference across it, then any phase angle limit may be expressed as a corresponding MW limit.

3.3. Generation constraints

In the short time available when islanding in response to a contingency it is not possible to start up generators. Generators that are operating can either have their input power disconnected, in which case their real output power drops to zero, or their output can be changed to a value within a small interval, $[P_g^{\text{G}-}, P_g^{\text{G}+}]$ say for generator g, around their pre-islanded value. The limits will depend on the ramp and output limits of the generator, and the amount of immediate or short-term reserve capacity available to the generator. This alternative operating regime is modelled by the constraint

$$\zeta_g P_g^{\text{G}-} \leq p_g^{\text{G}} \leq \zeta_g P_g^{\text{G}+}, \tag{6}$$

where ζ_g is a binary variable. If $\zeta_g = 0$ then generator g is switched off and $p_g^{\text{G}} = 0$; otherwise $\zeta_g = 1$ and its output is $p_g^{\text{G}} \in [P_g^{\text{G}-}, P_g^{\text{G}+}]$.

3.4. Load shedding

Because of the limits on generator power outputs and network constraints it may not be possible after islanding to fully supply all loads. It is therefore necessary to permit some shedding of loads. Note that this is *intentional* load shedding, not automatic shedding as a result of low voltages or frequency. To implement this in the real network there has to be central control over equipment.

Suppose that a load $d \in \mathcal{D}$ has a constant real power demand P_d^{D}. It is assumed that this load may be reduced by disconnecting a proportion $1 - \alpha_d$, where $0 \leq \alpha_d \leq 1$, so the load delivered is

$$p_d^{\mathrm{D}} = \alpha_d P_d^{\mathrm{D}}. \tag{7}$$

3.5. Objective function

The overall goal in islanding is to split the network and leave it in a secure steady state while maximizing the expected value of the load supplied. Suppose a reward M_d per unit is associated with the supply of load d. However if this load is part of Section 0, then because this section is vulnerable, it is assumed there is a risk of not being able to supply power to that load. Accordingly, a load loss penalty $0 \leq \beta_d < 1$ is defined, which may be interpreted as the probability of being able to supply a load d if placed in section 0. If d is placed in Section 1, a reward M_d is realized per unit supply, but if d is placed in Section 0 a lower reward of $\beta_d M_d < M_d$ is realized. The expected value of the load supplied is J_{DC}:

$$J_{\mathrm{DC}} = \sum_{d \in \mathcal{D}} M_d P_d (\beta_d \alpha_{0d} + \alpha_{1d}),$$

where,

$$\alpha_d = \alpha_{0d} + \alpha_{1d}, \forall d \in \mathcal{D}, \tag{8a}$$

$$0 \leq \alpha_{0d} \leq 1, \forall d \in \mathcal{D}, \tag{8b}$$

$$0 \leq \alpha_{1d} \leq \gamma_b, \forall b \in \mathcal{B}, d \in \mathcal{D}_b. \tag{8c}$$

Here a new variable α_{sd} is introduced for the load d delivered in Section $s \in \{0, 1\}$. If $\gamma_b = 0$, (and so the load at bus b is in Section 0), then $\alpha_{1d} = 0, \alpha_{0d} = \alpha_d$ and the reward is $\beta_d M_d P_d \alpha_d$. On the other hand, if $\gamma_b = 1$ then $\alpha_{1d} = \alpha_d$ and $\alpha_{0d} = 0$, giving a higher reward $M_d P_d \alpha_d$. Thus maximizing J_{DC} gives a preference for $\gamma_b = 1$ and a smaller section 0.

The DC optimal islanding problem with objective of maximizing J_{DC} usually has multiple feasible solutions with objectives close to the optimal value. This flexibility is exploited by introducing two penalty terms to the objective which are small enough not to affect significantly the primary objective, but improve the computational performance and provide the flexibility to guide the search towards solutions with good dynamic behaviour. The modified objective is to maximize

$$J_{\mathrm{DC}} - \varepsilon_1 \sum_{l \in \mathcal{L} \setminus \mathcal{L}^0} W_l (1 - \rho_l) - \varepsilon_2 \sum_{g \in \mathcal{G}} W_g (1 - \zeta_g) \tag{9}$$

where the W_l, ε_1, W_g and ε_2 are non-negative weights. The value of J_{DC} in the optimal is denoted by J^*_{DC}. The penalties discourage the disconnection of healthy lines and generators, *i.e.* they encourage the binary variables ρ_l and ζ_g to take the integer values 1 in the LP relaxations. This improves computational efficiency by reducing the size of the branch and bound tree.

A uniform weight, *e.g.*, $W_l = 1, \forall l$, will discourage equally all line cuts, while cuts to high-flow lines may be more heavily discouraged with $W_l = s_l^{\mathrm{L0}}$, where s_l^{L0} is the pre-islanding apparent power flow through the line. Generation disconnection is uniformly penalized by setting W_g equal to the generator's capacity P_g^{Gmax}.

3.6. Overall formulation

The overall formulation for islanding is to maximize (9) subject to constraints (1) to (8). The resulting problem is a MILP.

4. Post-islanding AC optimal load shedding

The solution of the DC islanding optimization includes values for loads shed and generator real outputs. In general, however, because these values come from a linearized model that ignores voltage and reactive power, these values will not be exactly optimal or feasible for the true AC problem. Therefore, to determine a good feasible AC solution for the islanded network, an AC optimal load shedding (OLS) problem is solved after the islanding optimization using the islands and generator disconnections determined by the DC islanding.

The AC-OLS optimization problem has the same form a standard OPF problem except that the objective is to maximize the expected value of load supplied. The AC-OLS is solved for the network in its islanded state. That is, the set $\mathcal{L}$ is modified by removing lines for which $\rho_l = 0$. Furthermore, any generator for which $\zeta_g = 0$ has its upper and lower bounds on real power set to zero; others are free to vary real power output within a restricted region, as described previously.

The problem is to maximize the total value of real power supplied to the loads:

$$J^*_{\text{AC}} = \max \sum_{d\in\mathcal{D}} R_d \alpha_d P_d, \tag{10}$$

subject to,

$$f(x) = 0, \tag{11a}$$

$$g(x) \leq 0, \tag{11b}$$

$$(p^{\text{G}}_g, q^{\text{G}}_g) \in \mathcal{O}_g, \forall g \in \mathcal{G}, \tag{11c}$$

$$(p^{\text{D}}_d, q^{\text{D}}_d) = \alpha_d (P^{\text{D}}_d, Q^{\text{D}}_d), \forall d \in \mathcal{D}. \tag{11d}$$

Here, R_d is the reward for supplying load d, and is equal to M_d if the load has been placed in Section 1 and $\beta_d M_d$ if placed in Section 0. The equality constraint (11a) captures Kirchhoff's current and voltage laws in a compact form; x denotes the collection of bus voltages, angles, and real/reactive power injections across the islanded network. The inequality constraint (11b) captures line limits and bus voltage limits.

The set $\mathcal{O}_g$ is the post-islanding region of operation for generator g, and depends on the solution of the islanding optimization and pre-islanded outputs of the generator. If $\zeta_d = 1$ the unit remains fully operational, and its output may vary within some region around the pre-islanded operating point; most generally $(p^{\text{G}}_g, q^{\text{G}}_g) \in \mathcal{O}_g(p^{\text{G0}}_g, q^{\text{G0}}_g)$, where $(p^{\text{G0}}_g, q^{\text{G0}}_g)$ is the pre-islanding operating point and $\mathcal{O}_g$ is defined by the output capabilities of the generating unit. If real and reactive power are independent, $p^{\text{G}}_g \in [P^{\text{G}-}_g, P^{\text{G}+}_g]$ and $q^{\text{G}}_g \in [Q^{\text{G}-}_g, Q^{\text{G}+}_g]$. If, conversely, $\zeta_g = 0$, then real power output is set to zero: $p^{\text{G}}_g = 0$. In that case, the unit may remain electrically connected to the network, with reactive power output free to vary within some specified interval $[Q^{\text{G}-}_g, Q^{\text{G}+}_g]$. Each load is assumed to be homogeneous, *i.e.* real and reactive components are shed in equal proportions.

The AC-OLS is a nonlinear programming (NLP) problem and may be solved efficiently by interior point methods.

Table 1: Pre- and post-islanding generator outputs for the 24-bus test example.

Bus		1	2	7	13	14	15	16	18	21	22	23
p^{G} (MW)	Pre	184	184	211	236	0	167	155	400	400	300	660
	Post	184	184	216	224	0	164	155	400	400	300	660
q^{G} (MVAr)	Pre	7	4	49	98	115	110	80	73	-8	-39	46
	Post	71	19	66	100	137	110	76	53	96	1	38

5. Computational results

This section presents computational results using the above islanding formulation. First, a demonstration is given of the islanding approach on a 24-bus network. Following that, the construction of the further test problems is described, then computation times for different convergence criteria for the MILP islanding calculation is given, and finally the accuracy of the DC solutions are assessed by comparing them with the AC solutions.

5.1. 24-bus network case study

The IEEE Reliability Test System [23] network comprises 38 lines and 24 buses, 17 of which have loads attached. Total generation capacity is 3405 MW from 32 synchronous generators. The total load demand is 2850 MW.

The islanding scenario is described as follows. With the network operating initially at a state determined from an AC OPF, it is suspected that bus 9 has a fault, and it is decided to island this bus to avoid further failures; hence, bus 9 is assigned to $\mathcal{B}^0$. It is assumed that $\beta_d = 0.75, \forall d \in \mathcal{D}$. In obtaining a new steady-state solution for the islanded network, each generator is permitted to varying real power output by up to 5% of its pre-islanding value, or switch off. In the objective, a unity reward, $R_d = 1$, is assumed for each load, and small penalties are placed on line cuts and generator disconnections ($\varepsilon_1 = 0.001$, $W_l = 1$, $\varepsilon_2 = 0.01$, $W_g = P_g^{\mathrm{Gmax}}$ in (9)).

Figure 2 shows the optimal islanding solution, obtained by solving the DC MILP islanding problem. Table 1 shows the real and reactive power outputs at each generator bus, both prior to, and after, islanding. All individual unit outputs are within limits. Table 2 shows the objective

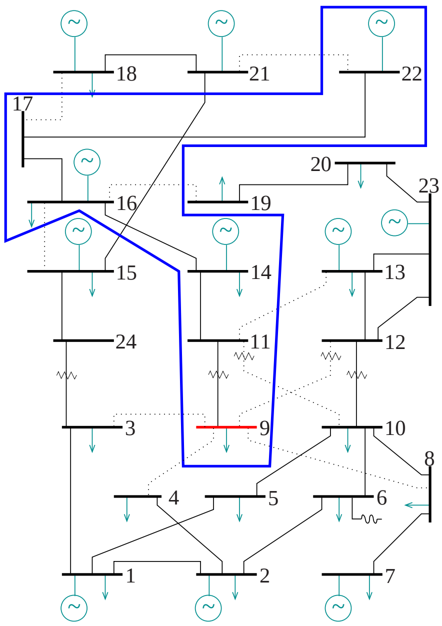

Figure 2: Islanding of the 24-bus network.

value—the expected load supply—and total values of generation and load for the DC islanding solution, and compares these values with those obtained from the post-islanding AC OLS. Buses 9, 11, 14, 16, 17 and 22 have been placed in section 0. No generators have been switched off. Of the original 2850 MW demand, 469 MW has been placed in the "risky" section 0, and 34.58 MW of load has been shed (as determined by the AC OLS). The returned AC OLS solution is feasible with respect to system line flow limits and all voltages are between 0.95 and 1.05 p.u.

Note that islanding bus 9 alone would have resulting in the loss of the entire 175 MW load at that bus, plus further possible losses in section 1 in order to balance the system. The optimized solution places more buses and loads in section 0 than is strictly necessary, but allows balanced, feasible islands to be obtained with minimum expected load shed.

5.2. *Further islanding test cases*

A set of islanding test cases was built based on test networks with between 9 and 300 buses. For a network with n^{B} buses, n^{B} scenarios were generated by assigning in turn each single bus to $\mathcal{B}^0$. No assignments were made to $\mathcal{B}^1$.

The possible post-islanding range of outputs for generator g when it is generating were defined

Table 2: Comparison of DC islanding and post-islanding AC OLS solutions for the 24-bus network.

	DC MILP	AC OLS
Objective (9)	2712.29	2706.81
Penalties	0.01	0.00
Exp. load supply, J^*_{DC} or J^*_{AC} (MW)	2712.30	2706.81
Generation (MW)	2863.57	2886.54
Load supplied (MW)	2822.73	2815.42
Load shed (MW)	27.27	34.58

as

$$[P_g^{\mathrm{G}-}, P_g^{\mathrm{G}+}] = [P_g^{\min}, P_g^{\max}] \cap [p_g^{\mathrm{G}0} - R_g^{\mathrm{G}}, p_g^{\mathrm{G}0} + R_g^{\mathrm{G}}],$$

where $P_g^{\min}$ and $P_g^{\max}$ are the minimum and maximum steady-state limits when generating, $p_g^{\mathrm{G}0}$ is the pre-islanding generation and R_g^{G} is the limit on change of output owing to ramp rate limits and/or generator reserve. For the 24-bus network, for which ramp rates are given, R_g^{G} is set to the maximum change over 2 minutes. For all other networks R_g^{G} is set to equal to 5% of $p_g^{\mathrm{G}0}$. The pre-islanding generation levels are those obtained by solving an AC OPF.

Where no line limits are present for a network, a maximum phase angle difference of 0.4 rad is imposed for each line. In the objective function, a value of 0.75 is used for the load loss penalty β_d, while the values of ε_1 and ε_2 in (9)—the penalties on line cuts and generator disconnection respectively—are 0.1 and 0.0001, with $W_l = 1$ and $W_g = P_g^{\mathrm{G}+}$.

5.3. Computation times and optimality

The speed with which islanding decisions have to be made depends on whether the decision is being made *before* a fault has occurred, as part of contingency planning within secure OPF, or *after*, in which case the time scale depends on the cause of the contingency. Especially in the second case it is important to be able to produce feasible solutions within short time periods even if these are not necessarily optimal. Results are therefore presented for a range of optimality tolerances: 'feasible' *i.e.* first integer feasible solution found, and relative MIP gaps of 5%, 1% and 0%.

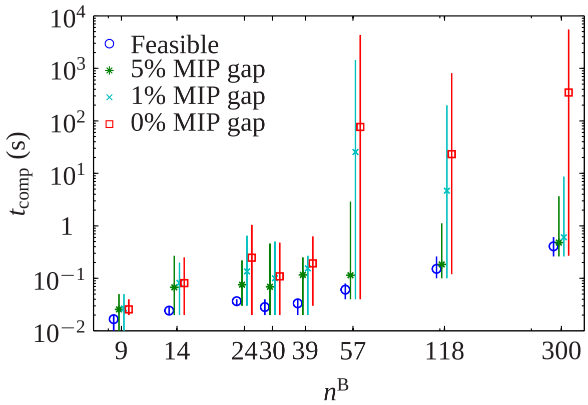

Figure 3: Mean, max and min times for finding, to different levels of optimality, islanding solutions for different test networks.

Problems were solved on a dual quad-core 64-bit Linux machine with 8 GiB RAM, using AMPL 11.0 with parallel CPLEX 12.3 to solve MILP problems. Computation times quoted include only the time taken to solve the islanding optimization to the required level of optimality, and not the AC-OLS, and are obtained as the elapsed (wall) time used by CPLEX during the `solve` command. A time limit of 5000 seconds is imposed.

Figure 3 shows the times required to find obtain feasible islanding solutions to varying proven levels of optimality. Minimum, mean and maximum times are obtained for each network by solving each of the n^B scenarios once. The first set of times show that all problems are solved to feasibility well within 1 s. In all cases, a feasible solution was found at the root note, without requiring branching.

For a MILP problem solved by branch and bound, the optimal integer solution is bounded from below (for maximization) by the highest integer objective value found so far during the solution process, and from above by the maximum objective of the relaxed solution among all leaf nodes of the tree. The relative MIP gap is the relative error between these two bounds. Figure 3 indicates the progress made by the CPLEX solver, in terms of the times required to reach relative MIP gaps of 5%, 1% and 0% (*i.e.*, optimality) respectively. Performance is very promising for solving to 5%, with all problems solved to this tolerance within five seconds. Times to 1% and 0% gaps are of the same order for the smaller networks (up to 39 buses), but the 57-, 118- and 300-bus networks can taken significantly longer to solve to these tolerances.

Table 3: Relative errors (%) between optimal and returned solutions.

	Feasible	5% gap	1% gap
Min	0.00	0.00	0.00
Mean	8.57	0.42	0.04
Max	25.00	3.86	0.80

Table 3 shows the means of the relative errors between the solution value returned at termination of the solver and the actual optimum, where this has been obtained by solving the problem to full optimality (0%). The actual gaps between early termination solutions and the true optima are nearer zero than the 5% or 1% bounds. Therefore, good islanding solutions with respect to the DC model can be provided even when the solver is terminated early and moreover these solutions can be found quickly. Moreover, because the DC model is an approximation of the AC model, there is little advantage in solving it to proven optimality.

5.4. *Feasibility and accuracy of DC islanding solution*

The post-islanding AC-OLS showed that some of the islanding solutions were AC infeasible, *i.e.*, there was no solution to the AC-OLS lying within normal voltage bounds. Relaxing the normal voltage bounds by an extra 0.06 p.u. gave a solution in all cases; however, this is not always possible for practical networks.

It was noted that in many of these AC-infeasible cases, there was sufficient global reactive power capacity in each island. However, reactive power and voltage is a local problem, and hence achieving a global reactive power balance is not sufficient to ensure a normal voltage profile. This is an issue that is overlooked by most controlled islanding schemes, and instead it is assumed that reactive power can be compensated locally. This is not always a justifiable assumption, however, and further research is needed on methods for obtaining, directly, islands with a healthy voltage profile.

Table 4 gives the number of these AC-infeasible cases as well as the number that did not solve to 0% optimality gap within 5000 seconds. For all the remaining cases the differences between the objectives as predicted by the DC islanding optimization and the actual value from post-islanding

Table 4: Number of unique problems included in the comparisons.

n^{B}	9	14	24	30	39	57	118	300
MIP gap > 0%	0	0	0	0	0	1	1	17
Voltage infeasible	0	2	7	7	9	6	17	72
Cases compared	9	12	17	23	30	50	100	211

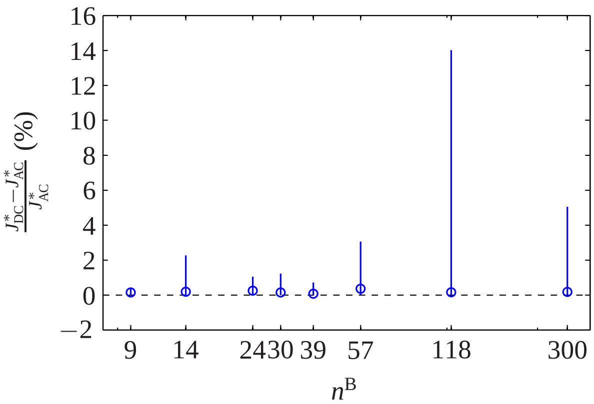

Figure 4: Mean, max and min relative errors between DC and AC objective values.

AC-OLS was calculated as is shown in Figure 4. The adopted islanding solution in each case is that from solving the problem to full optimality.

The comparison in Figure 4 shows how well the DC model predicts the AC objective. There are a few cases where the DC objective is a significant over-estimate, however on average the objective values are within 0.3%.

6. Dynamic stability

Solving the MILP islanding problem and, subsequently, the AC-OLS provides a feasible steady-state operating point for the network in its post-islanding configuration. Since the objective minimizes the load shed and the constraints limit the changes to generator outputs, the proposed solution will naturally limit, to some extent, the disruption to the system power flows. Nevertheless, since neither the transient response is modelled when designing islands nor the generators are necessarily grouped according to coherent modes, it is possible that the islanding actions may lead

Table 5: Results of time-domain simulations with original line-cut and generator penalties.

n^{B}	9	14	24	30	39	57	118	300
Cases compared	9	12	17	23	30	50	100	211
Unstable	0	0	1	0	0	0	1	12
Stable	9	12	16	23	30	50	99	199

to dynamic instability. This section therefore describes the use of a time-domain simulation to investigate this issue. Results are presented for the previous 9- to 300-bus islanding cases to test whether or not the act of islanding induces dynamic instability.

Time-domain simulations for all of the islanding scenarios described in Sec. 5.3 were performed using PSAT [24]. Second-order non-linear models of synchronous machine dynamics were used with machine parameters taken from [25], with a damping coefficient $D = 0.5$. The loads were assume to have no dynamics. In practice the damper windings and the control systems (turbine governor, AVR) would act to dampen the oscillations more than in the simulation making the real system more stable than in the simulations. Each simulation is started from an undisturbed pre-islanding operating point, at which all generators have an angular frequency of 1 p.u. and the network is balanced.

The results are given in Table 5. In total, 14 out of 452 islanding solutions were found to lead to instability. Investigation of the individual cases found that, in all cases, severe transients were caused by cuts to high-flow lines. However, re-solving the islanding optimizations with increased penalties on high-flow lines ($W_l = s_l^{\mathrm{L0}}$ and $\varepsilon_1 = 10^{-4} \sum_d P_d^{\mathrm{D}}$) and switching-off of generators ($W_g = P_g^{\mathrm{G+}}$ and $\varepsilon_2 = 1$) resulted in all cases being stable.

As expected these larger penalty coefficients caused a drop in the primary DC objective value, J_{DC}^*. However Table 6 shows that this degradation is small, and is an acceptable trade-off for removing all of the unstable cases. As an added advantage, as Figure 5 shows, solve times for the larger networks are shorter with the heavier penalties.

Table 6: Decrease in objective J^*_{DC} (%) for line-cut and generator penalties increased versus previous penalties.

n^{B}	9	14	24	30	39	57	118	300
Min	0.00	0.00	0.00	0.00	0.00	0.00	0.00	0.00
Mean	0.16	0.78	0.59	0.03	0.34	0.06	0.20	0.46
Max	0.48	10.85	2.87	0.68	5.09	1.00	2.70	7.03

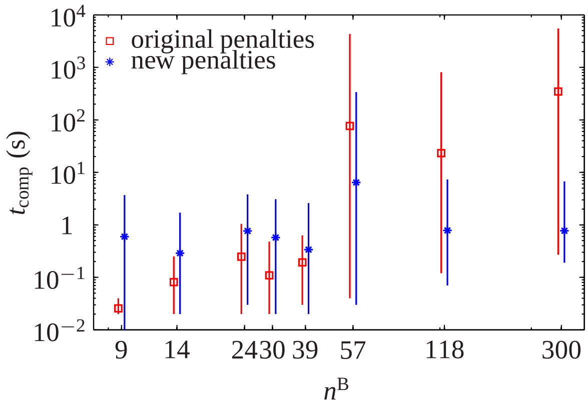

Figure 5: Mean, max and min solve times to optimality with original penalties ($\varepsilon_1 = 0.1$, $W_l = 1$, $\varepsilon_2 = 10^{-4}$, $W_g = P_g^{\mathrm{G+}}$) and new penalties ($\varepsilon_1 = 10^{-4}\sum_d P_d^{\mathrm{D}}$, $W_l = s_l^{\mathrm{L0}}$, $\varepsilon_2 = 1$, $W_g = P_g^{\mathrm{G+}}$).

7. Conclusions

In this paper, an optimization-based approach to controlled islanding and intentional load shedding has been presented. The proposed method uses MILP to determine which lines to cut, loads to shed, and generators to switch or adjust in order to isolate an uncertain or failure-prone region of the network. The optimization framework allows linear network constraints—a loss-modified DC power flow model, line limits, generator outputs—to be explicitly included in decision making, and produces balanced, steady-state feasible DC islands. AC islanding solutions are found via the subsequent solving of an AC optimal load shedding problem. The dynamic stability of resulting islanding solutions is assessed via time-domain simulation.

The approach has been demonstrated through examples on a range of test networks, and the practicality of the method in terms of computation time has been demonstrated. Good feasible islanding solutions can be found very quickly. While the dynamic response is not explicitly modelled in the optimizations, time-domain simulations of the islanding solutions have indicated that instability is avoided by appropriate choices of penalties on cuts to high-flow lines and disconnections of generating units, both of which discourage disruption to the network. Furthermore, it was shown that these penalties had a small effect on the amount of load required to be shed.

This paper has also served to raise the issue of ensuring adequate reactive power and a healthy voltage profile after controlled islanding, and issue overlooked by most approaches, which instead assume that reactive power may be compensated locally. Further research is needed in this area.

Future research will investigate the inclusion of constraints for dynamic stability in the problem, the generalization of the method to partitioning the system following slow coherency analysis, and the modelling of reactive power in the optimization to ensure a healthy voltage profile.

Acknowledgements

The authors would like to thank Professor Janusz Bialek and Dr Patrick McNabb of the School of Engineering and Computing Sciences, Durham University for helpful discussions on power system dynamics.

References

[1] Final Report of the Investigation Committee on the 28 September 2003 Blackout in Italy, Final Report, Union for the Coordination of the Transmission of Electricity (UCTE), 2004.

[2] S. Larsson, A. Danell, The black-out in southern Sweden and eastern Denmark, September 23, 2003, in: IEEE Power Systems Conference and Exposition, 2006.

[3] U.S.-Canada Power System Outage Task Force, Final Report on the August 14, 2003 Blackout in the United States and Canada: Causes and Recommendations, Final Report, URL https://reports.energy.gov/, 2004.

[4] Final Report System Disturbance on 4 November 2006, Final Report, Union for the Coordination of the Transmission of Electricity (UCTE), 2007.

[5] Report of the National Grid Investigation into the Frequency Deviation and Automatic Demand Disconnection that occurred on the 27th May 2008, Final Report, National Grid, 2009.

[6] J. W. Bialek, Are blackouts contagious?, IEE Power Engineer 17 (6) (2003) 10.

[7] J. W. Bialek, Blackouts in the US/Canada and continental Europe in 2003: is liberalisation to blame?, in: IEEE PowerTech Conference, Russia, 2005.

[8] G. Andersson, P. Donalek, R. Farmer, N. Hatziargyriou, I. Kamwa, P. Kundur, N. Martins, J. Paserba, P. Pourbeik, J. Sanchez-Gasca, R. Schulz, A. Stankovic, C. Taylor, V. Vittal, Causes of the 2003 Major Grid Blackouts in North America and Europe, and Recommended Means to Improve System Dynamic Performance, IEEE Transactions on Power Systems 20 (4) (2005) 1922–1928.

[9] D. E. Newman, B. A. Carreras, M. Kirchner, I. Dobson, The Impact of Distributed Generation on Power Transmission Grid Dynamics, in: 44th Hawaii International Conference on System Science, 2011.

[10] B. Yang, V. Vittal, G. T. Heydt, Slow-Coherency-based Controlled Islanding—A Demonstration of the Approach on the August 14, 2003 Blackout Scenario, IEEE Transactions on Power Systems 21 (2006) 1840–1847.

[11] K. Sun, D.-Z. Zheng, Q. Lu, Splitting Strategies for Islanding Operation of Large-Scale Power Systems Using OBDD-Based Methods, IEEE Transactions on Power Systems 18 (2003) 912–923.

[12] H. You, V. Vittal, X. Wang, Slow Coherency-Based Islanding, IEEE Transactions on Power Systems 19 (1) (2004) 483–491.

[13] X. Wang, V. Vittal, System Islanding using Minimal Cutsets with Minimum Net Flow, in: IEEE Power Systems Conference and Exposition, 2004.

[14] G. Xu, V. Vittal, Slow Coherency Based Cutset Determination Algorithm for Large Power Systems, IEEE Transactions on Power Systems 25 (2) (2010) 877–884.

[15] L. Liu, W. Liu, D. A. Cartes, I.-Y. Chung, Slow coherency and Angle Modulated Particle Swarm Optimization based islanding of large-scale power systems, Advanced Engineering Informatics 23 (1) (2009) 45–56.

[16] M. R. Aghamohammadi, A. Shahmohammadi, Intentional islanding using a new algorithm based on ant search mechanism, International Journal of Electrical Power and Energy Systems 35 (2012) 138–147.

[17] M. Jin, T. S. Sidhu, K. Sun, A New System Splitting Scheme Based on the Unified Stability Control Framework, IEEE Transactions on Power Systems 22 (1) (2007) 433–441.

[18] C. G. Wang, B. H. Zhang, Z. G. Hao, J. Shu, P. Li, Z. Q. Bo, A Novel Real-Time Searching Method for Power System Splitting Boundary, IEEE Transactions on Power Systems 25 (4) (2010) 1902–1909.

[19] D. Bienstock, S. Mattia, Using mixed-integer programming to solve power grid blackout problems, Discrete Optimization 4 (2007) 115–141.

[20] E. B. Fisher, R. P. O'Neill, M. C. Ferris, Optimal Transmission Switching, IEEE Transactions on Power Systems 23 (3) (2008) 1346–1355.

[21] A. Khodaei, M. Shahidehpour, Security-constrained transmission switching with voltage constraints, International Journal of Electrical Power and Energy Systems 35 (2012) 74–82.

[22] P. A. Trodden, W. A. Bukhsh, A. Grothey, K. I. M. McKinnon, MILP formulation for islanding of power networks, Tech. Rep. ERGO 11-015, Edinburgh Research Group in Optimization, School of Mathematics, Univer-

sity of Edinburgh, 2011.

[23] Reliability Test System Task Force of the Application of Probability Methods Subcommittee, IEEE Reliability Test System, IEEE Transactions on Power Apparatus and Systems PAS-98 (6) (1979) 2047–2054.

[24] F. Milano, Documentation for PSAT version 2.0.0, University of Castilla – La Mancha, 2008.

[25] Reliability Test System Task Force of the Application of Probability Methods Subcommittee, IEEE Reliability Test System – 1996, IEEE Transactions on Power Systems 14 (3) (1999) 1010–1020.